Enzyme therapy in mannose receptor-null mucopolysaccharidosis VII mice defines roles for the mannose 6-phosphate and mannose receptors

William S. Sly*†, Carole Vogler‡, Jeffrey H. Grubb*, Beth Levy‡, Nancy Galvin‡, Yun Tan*, Tatsuo Nishioka§, and Shunji Tomatsu§

*Edward A. Doisy Department of Biochemistry and Molecular Biology, Departments of ‡Pathology and §Pediatrics, Saint Louis University School of Medicine, 1402 South Grand Boulevard, St. Louis, MO 63104

Contributed by William S. Sly, August 14, 2006

Enzyme replacement therapy (ERT) is available for several lysosomal storage diseases. Except for Gaucher disease, for which an enzyme with exposed mannosyl residues targets mannose receptors (MR) on macrophages, ERT targets primarily the mannose 6-phosphate receptor (MPR). Most recombinant lysosomal enzymes contain oligosaccharides with both terminal mannosyl and mannose 6-phosphate residues. Effective MPR-mediated delivery may be compromised by rapid clearance of infused enzyme by the MR on fixed tissue macrophages, especially Kupffer cells. To evaluate the impact of this obstacle to ERT, we introduced the MR-null mutation onto the mucopolysaccharidosis type VII (MPS VII) background and produced doubly deficient $MR^{-/-}$ MPS VII mice. The availability of both $MR^{+/+}$ and $MR^{-/-}$ mice allowed us to study the effects of eliminating the MR on MR- and MPR-mediated plasma clearance and tissue distribution of infused phosphorylated (P) and nonphosphorylated (NP) forms of human β-glucuronidase (GUS). In $MR^{+/+}$ MPS VII mice, the MR clearance system predominated at doses up to 6.4 mg/kg P-GUS. Genetically eliminating the MR slowed plasma clearance of both P- and NP-GUS and enhanced the effectiveness of P-GUS in clearing storage in kidney, bone, and retina. Saturating the MR clearance system by high doses of enzyme also improved targeting to MPR-containing tissues such as muscle, kidney, heart, and hepatocytes. Although ablating the MR clearance system genetically is not practical clinically, blocking the MR-mediated clearance system with high doses of enzyme is feasible. This approach delivers a larger fraction of enzyme to MPR-expressing tissues, thus enhancing the effectiveness of MPR-targeted ERT.

β-glucuronidase deficiency | immune tolerance | lysosomal storage disease

The mucopolysacchridoses (MPS) are a group of lysosomal storage diseases (LSDs) in which a deficiency of one or more lysosomal enzymes interferes with the degradation of glycosaminoglycans (GAGs), resulting in their storage in the lysosome. Accumulated GAG storage in lysosomes results in progressive cellular and organ dysfunction (1). In recent years, advances have been made in the treatment of several LSDs (2–5). In these diseases, lysosomal storage can be partially or completely reversed in many target tissues by i.v. infusion of the missing lysosomal enzyme. Traditionally, it was assumed that lysosomal enzymes would be delivered to target tissues so long as the enzymes contained the mannose 6-phosphate (M6P) recognition marker (6). However, other factors can influence the delivery of lysosomal enzymes to target tissues. Among these is the presence of nonphosphorylated oligosaccharides on the enzymes and the extent to which these have been processed from high mannose to complex-type oligosaccharides (7). The latter determines the number of exposed mannose residues on the enzyme, which can target the enzyme preferentially to the mannose receptor (MR). In addition, the distribution of the MR and the mannose 6-phosphate receptor (MPR) and their relative abundance in target tissues affect cells targeted by infused enzyme (6).

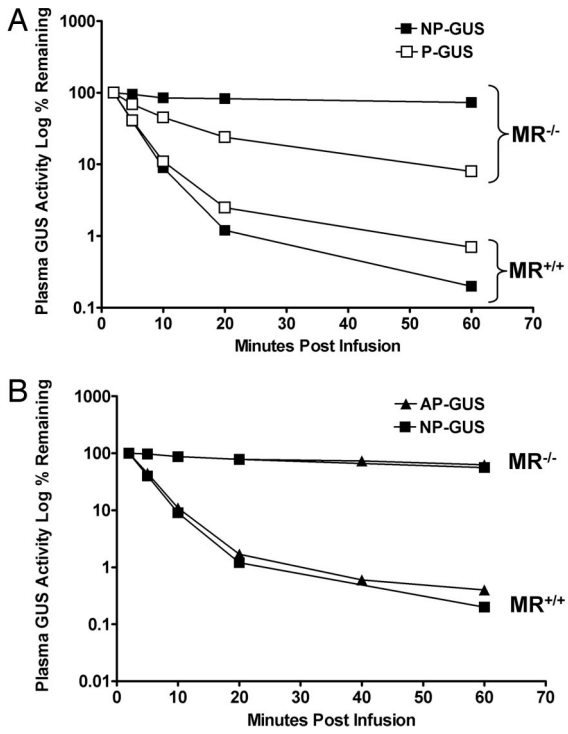

Fig. 1. Plasma clearance of P- and NP-GUS (*A*) or AP- and NP-GUS (*B*) in $MR^{-/-}$ and $MR^{+/+}$ mice. (*A*) P- (□) and NP-GUS (■) were infused at a dose of 0.2 mg/kg and plasma GUS levels measured over the next hour. Note that the NP-GUS in the $MR^{+/+}$ mice was very rapidly cleared (AUC = 411 units/h per ml) in contrast to the much slower clearance in $MR^{-/-}$ mice (AUC = 4,703 units/h per ml). P-GUS is also rapidly cleared in the $MR^{+/+}$ mice (AUC = 473 units/h per ml) but shows an intermediate rate of clearance in $MR^{-/-}$ mice (AUC = 1,524 units/h per ml), reflecting the M6P-mediated clearance in the absence of MR. (*B*) Clearance rates of AP-GUS (▲) (AUC = 4,395 units/h per ml) and NP-GUS (■) (AUC = 4,703 units/h per ml) appear nearly equivalent in $MR^{-/-}$ mice.

The murine model of MPS VII has been used successfully to study many different therapies for lysosomal storage diseases, including enzyme replacement therapy (ERT; ref. 8). We have

Author contributions: W.S.S., C.V., J.H.G., T.N., and S.T. designed research; J.H.G., B.L., N.G., Y.T., T.N., and S.T. performed research; N.G., Y.T., and T.N. contributed new reagents/analytic tools; W.S.S., C.V., J.H.G., B.L., and S.T. analyzed data; and W.S.S., C.V., and J.H.G. wrote the paper.

The authors declare no conflict of interest.

Abbreviations: MR, mannose receptor; MPR, mannose 6-phosphate receptor; M6P, mannose 6-phosphate; ERT, enzyme replacement therapy; MPS, mucopolysaccharidosis; GUS, β-glucuronidase; hGUS, human GUS; P-GUS, phosphorylated GUS; NP-GUS, nonphosphorylated GUS; AUC, area under the curve; AP, alkaline phosphatase.

†To whom correspondence should be addressed. E-mail: slyws@slu.edu.

www.pnas.org/cgi/doi/10.1073/pnas.0607053103

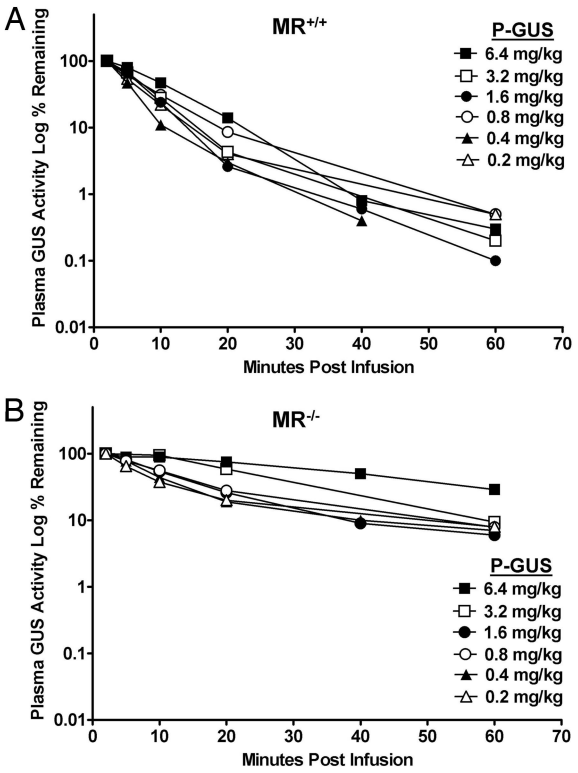

Fig. 2. Effect of increasing dose of P-GUS on plasma clearance in $MR^{+/+}$ (*A*) and $MR^{-/-}$ (*B*) mice. P-GUS was infused at doses of 0.2, 0.4, 0.8, 1.6, 3.2, and 6.4 mg/kg, and plasma GUS levels measured over the next hour. At the two highest doses in $MR^{-/-}$ mice (*B*), clearance was slower than at lower doses and much slower than in all doses in $MR^{+/+}$ mice (*A*), reflecting the rapid clearance by the MR in $MR^{+/+}$ mice and the saturation of the MPR with the higher doses in $MR^{-/-}$ mice.

modified this model by making it immunologically tolerant to human β-glucuronidase (hGUS; ref. 9). This reduces the risk of complications from an immune response when hGUS is infused repeatedly in ERT.

Recently, another useful murine model has been developed in which the MR has been knocked out (10). We bred this strain on to the B6 MPS VII/E540A^{Tg} background to produce a model that is mouse GUS-deficient, hGUS-tolerant, and MR-deficient (MPS VII/$MR^{-/-}$). In the current studies, we used both the MPS VII/E540A^{Tg} $MR^{+/+}$ (referred to later as $MR^{+/+}$) and the MPS VII/E540A^{Tg} $MR^{-/-}$ (referred to later as $MR^{-/-}$) mice to study the individual roles of the MPR and the MR in enzyme therapy.

Results

Effect of the MR on Clearance of Low-Dose Phosphorylated (P)-GUS vs. Nonphosphorylated (NP)-GUS. We compared the plasma clearance of infused P-GUS with that of NP-GUS (both at 0.2 mg/kg) in $MR^{+/+}$ and $MR^{-/-}$ MPS VII mice (Fig. 1*A*). Both were cleared at approximately the same initial rate ($t_{1/2}$ of ≈5 min) in $MR^{+/+}$ mice. In contrast, the clearance of infused P-GUS in $MR^{-/-}$ mice was significantly prolonged ($t_{1/2}$ of ≈9 min). Markedly slower still was the clearance of NP-GUS in the $MR^{-/-}$ mice ($t_{1/2}$ of ≈4 h). This experiment shows the contributions of both the MR and MPR in clearance of recombinant hGUS in the MPS VII mouse. Both systems contribute to the rapid clearance of P-GUS in the $MR^{+/+}$ mouse. The prolonged circulation of infused NP-GUS in the $MR^{-/-}$ mouse reflects the fact that neither receptor-mediated clearance system is operative. The more rapid clearance of P- than NP-GUS in the $MR^{-/-}$ mice shows the isolated effect of MPR-mediated clearance.

Table 1. Calculated AUC for plasma clearance of P-GUS in $MR^{+/+}$ and $MR^{-/-}$ mice infused with increasing doses of P-GUS

	Dose, mg/kg					
	0.2	0.4	0.8	1.6	3.2	6.4
$MR^{+/+}$	641	474	852	646	740	1,052
$MR^{-/-}$	1,351	1,347	1,740	1,513	2,918	3,589

AUC calculated from data in Fig. 2.

The dominant role of the MR in the clearance of both NP- and P-GUS is evident from Fig. 1*A*, as there was no difference in the areas under the curve (AUCs) for both enzymes in $MR^{+/+}$ mice over the first 60 min (see legend to Fig. 1*A*). Thus, at this dose, we could not demonstrate the impact of the MPR on enzyme clearance in $MR^{+/+}$ mice. The AUCs were increased for both P- and NP-GUS in the $MR^{-/-}$ mice compared with those for $MR^{+/+}$ mice. However, the AUC for P-GUS was increased only 4-fold, whereas that of NP-GUS was increased 10-fold. This difference indicates that, in the absence of the MR, the role of the MPR-mediated clearance can be readily demonstrated.

Sands *et al.* (6) showed that NP-GUS, produced in a baculovirus/insect cell expression system, contains oligosaccharides with terminal mannose residues that interact with the MR but not the MPR. To verify that more rapid clearance of P- than NP-GUS in the $MR^{-/-}$ mice was MPR-mediated, we dephosphorylated P-GUS with placental alkaline phosphatase (AP) and compared its clearance with that of NP-GUS. Fig. 1*B* shows that NP- and AP-GUS (both lacking M6P) showed similarly slowed clearance ($t_{1/2}$ of ≈4 h) in the $MR^{-/-}$ mice and similarly

Table 2. Tissue GUS levels 24 h after infusion of different doses of P-GUS in $MR^{+/+}$ and $MR^{-/-}$ mice

Tissue*	Dose, mg/kg	Tissue level, units/mg		$\frac{MR^{-/-}}{MR^{+/+}}$
		$MR^{+/+}$	$MR^{-/-}$	
Brain	0.4	0.10 ± 0.05	0.12 ± 0.04	1.20
	1.6	0.14 ± 0.04	0.20 ± 0.06	1.43
	6.4	0.34 ± 0.17	0.70 ± 0.10	2.06
Liver	0.4	87.6 ± 12.4	72.5 ± 12.1	0.83
	1.6	381 ± 20.3	324 ± 15.5	0.85
	6.4	1,577 ± 211	1,290 ± 181	0.82
Spleen	0.4	19.9 ± 2.2	12.4 ± 4.0	0.62
	1.6	145 ± 15	41.7 ± 9.0	0.29
	6.4	890 ± 298	198 ± 18	0.22
Heart	0.4	2.9 ± 1.2	4.0 ± 1.7	1.38
	1.6	6.8 ± 2.9	7.6 ± 0.7	1.12
	6.4	27.5 ± 6.3	63.5 ± 31	2.30
Kidney	0.4	3.1 ± 1.5	3.3 ± 1	1.06
	1.6	8.2 ± 3.2	11.0 ± 1.9	1.34
	6.4	19.9 ± 3.9	64.5 ± 18	3.2
Lung	0.4	4.0 ± 1.4	4.9 ± 0.9	1.2
	1.6	10.2 ± 5	11.2 ± 2.2	1.1
	6.4	33.2 ± 15	41.7 ± 9.1	1.3
Muscle	0.4	0.57 ± 0.19	0.85 ± 0.47	1.49
	1.6	1.02 ± 0.54	1.35 ± 0.65	1.32
	6.4	2.70 ± 1.77	17.2 ± 4.2	6.37
Bone (including marrow)	0.4	8.4 ± 6.1	6.6 ± 2.9	0.79
	1.6	35.0 ± 24	41.2 ± 32.1	1.17
	6.4	198 ± 137	196 ± 133	0.99
Plasma (units/ml)	0.4	1.41 ± 0.51	203 ± 69	144
	1.6	7.75 ± 4.25	890 ± 24	115
	6.4	36.8 ± 26.5	4,169 ± 734	113

*Tissues were collected after perfusion to remove enzyme in blood.

Table 3. Liver accumulation 1 h after infusion of $MR^{-/-}$ and $MR^{+/+}$ mice with 1 mg/kg P-GUS

Genotype	P-GUS, units infused*	Total P-GUS, units in liver*	Percent of infused enzyme in liver*
$MR^{-/-}$	120,900 ± 3,100	46,576 ± 3,189	38.5% ± 3.6
$MR^{+/+}$	107,467 ± 13,940	44,907 ± 5,736	41.8% ± 0.2

*Mean ± SD.

rapid clearance in the $MR^{+/+}$ mice, indicating they are equivalent ligands for the MR-mediated clearance system. In addition, this experiment shows that the more rapid clearance of P-GUS in the $MR^{-/-}$ mouse depends on the M6P recognition marker, which was destroyed by AP (11–13).

Effect of Increasing Dose on Clearance of P-GUS in the Presence or Absence of the MR. Even though P-GUS contains phosphorylated oligosaccharides, it also contains high-mannose oligosaccharides with exposed terminal mannoses (14). To determine what dose of P-GUS is required to saturate the MR vs. the MPR, we did an enzyme saturation curve at doses from 0.2 to 6.4 mg/kg P-GUS in $MR^{+/+}$ (Fig. 2*A*) and $MR^{-/-}$ (Fig. 2*B*) mice. In $MR^{+/+}$ mice, it was difficult to see saturation <6.4 mg/kg, at which the $t_{1/2}$ of clearance was prolonged to ≈10 min. Saturation of MPR-mediated clearance by P-GUS in $MR^{-/-}$ mice was evident at a lower dose. (Clearance $t_{1/2}$ was 23 min at 3.2 mg/kg and 42 min at 6.4 mg/kg.) This corresponds to 4- and 3.4-fold increases in AUC over the first 60 min for P-GUS at 3.2 and 6.4 mg/kg, respectively, in $MR^{-/-}$ mice (Table 1).

Effect of Increasing Dose of P-GUS on Its Tissue Distribution in the Presence or Absence of the MR. To address this question, we infused P-GUS at doses of 0.4, 1.6, or 6.4 mg/kg into $MR^{+/+}$ and $MR^{-/-}$ mice. In all mice, increasing the dose led to increased enzyme delivery (Table 2). In $MR^{-/-}$ mice, spleen, which normally depends largely on MR-mediated delivery, received only 20% of the enzyme seen in $MR^{+/+}$ mice at the highest doses. However, liver showed only slightly less enzyme in the $MR^{-/-}$ mice at all doses.

We then compared the fraction of total infused enzyme delivered to liver in $MR^{+/+}$ and $MR^{-/-}$ mice. After 1 h, 99% of the infused enzyme had been cleared in the $MR^{+/+}$ and 94% in the $MR^{-/-}$ mice. The fraction of administered enzyme in liver was 41.8 ± 0.2% in $MR^{+/+}$ mice and 38.6 ± 3.6% in $MR^{-/-}$ mice (Table 3). The surprisingly large amount of GUS still delivered to liver in the $MR^{-/-}$ mice suggests that nearly 40% of the total MPR accessible to infused P-GUS enzyme is contained in the liver.

In other tissues that express both the MR and MPR (such as lung and bone), there is also a dose-dependent increase in enzyme activity (Table 2). However, the amount of enzyme in these tissues is not greatly different between $MR^{-/-}$ and $MR^{+/+}$ mice regardless of dose. By contrast, heart, kidney, and muscle, which normally express the MPR but little or no MR, showed a greater increase with increasing dose in $MR^{-/-}$ than in $MR^{+/+}$

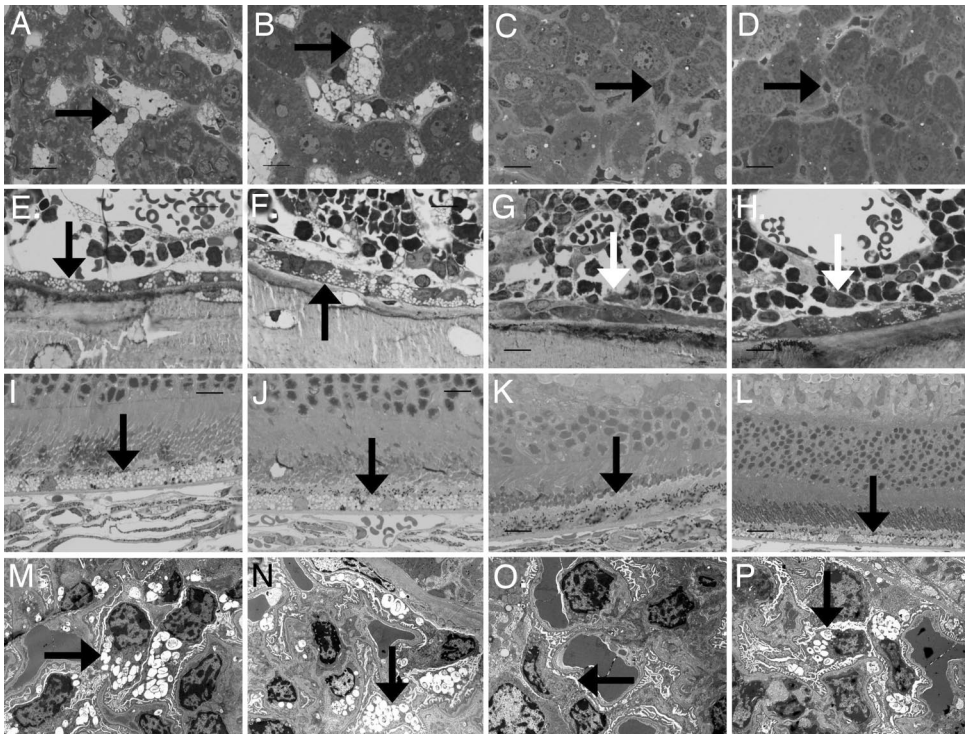

Fig. 3. Impact of three doses of 1 mg/kg P-GUS on lysosomal storage of P-GUS in liver, bone, retina, and kidney in $MR^{-/-}$ and $MR^{+/+}$ mice. (*A–D*) Compared with an untreated $MR^{-/-}$ mouse (*A*) and an untreated $MR^{+/+}$ mouse (*B*), both $MR^{-/-}$ (*C*) and $MR^{+/+}$ (*D*) treated mice had essentially complete clearance of lysosomal storage in the Kupffer cells in the liver (arrow) 1 wk after the last enzyme treatment. (*E* and *F*) The bone of untreated $MR^{-/-}$ (*E*) and $MR^{+/+}$ (*F*) mice had lysosomal storage in osteoblasts (arrow) and marrow sinus-lining cells. (*G* and *H*) Treated $MR^{-/-}$ (*G*) and $MR^{+/+}$ (*H*) mice had similar marked reduction in storage in the sinus-lining cells. However, only treated $MR^{-/-}$ mice (*G*) had a marked reduction in storage in the osteoblasts (arrow). Osteoblasts in treated $MR^{+/+}$ mice (*H*) had only a slight reduction in storage (arrow). (*I* and *J*) Untreated $MR^{-/-}$ (*I*) and $MR^{+/+}$ (*J*) mice had abundant lysosomal storage in retinal pigment epithelial cells (arrow). (*K* and *L*) In treated $MR^{-/-}$ mice (*K*), the retinal pigment epithelial cells had reduced storage. Treated $MR^{+/+}$ mice (*L*) showed minimal or no reduction in storage in the retinal pigment epithelial cells. (*M* and *N*) Untreated $MR^{-/-}$ (*M*) and $MR^{+/+}$ (*N*) mice both had marked lysosomal distention in the renal visceral epithelial cells (podocytes; arrow). (*O* and *P*) After ERT with P-GUS, $MR^{-/-}$ mice (*O*) showed a marked reduction in lysosomal storage in these cells, but treated $MR^{+/+}$ mice (*P*) showed much less treatment effect. (Scale bar: *A–L*, toluidine blue, 20 μm; *M–P*, uranyl acetate-lead citrate, 10 μm.)

Table 4. Tissue levels of GUS 7 days after third weekly infusion of P-GUS in $MR^{-/-}$ and $MR^{+/+}$ mice

Tissue	$MR^{-/-}$, units/mg protein				$MR^{+/+}$, units/mg protein			
	Noninfused		Plue enzyme*		Noninfused		Plus enzyme*	
	Triplicate mice	Mean ± SD	Triplicate mice	Mean ± SD	Triplicate mice	Mean ± SD	Triplicate mice	Mean ± SD
	0.06		0.11		0.06		0.07	
Brain	0.08	0.06 ± 0.01	0.12	0.10 ± 0.02	0.05	0.05 ± 0.004	0.07	0.07 ± 0.00
	0.05		0.08		0.05		0.07	
	0.30		88.14		0.34		79.20	
Liver	0.31	0.29 ± 0.02	70.73	84.1 ± 9.7	0.29	0.30 ± 0.03	74.78	70.9 ± 8.7
	0.27		93.54		0.26		58.95	
	0.16		10.27		0.08		15.84	
Spleen	0.27	0.23 ± 0.05	6.96	7.54 ± 2.03	0.12	0.13 ± 0.05	17.25	15.61 ± 1.44
	0.27		5.40		0.19		13.74	
	0.20		1.35		0.07		0.77	
Heart	0.21	0.17 ± 0.05	1.22	1.25 ± 0.07	0.05	0.06 ± 0.009	0.79	0.78 ± 0.009
	0.09		1.18		0.07		0.77	
	0.08		1.80		0.07		0.91	
Kidney	0.07	0.10 ± 0.03	0.85	1.32 ± 0.48	0.04	0.05 ± 0.02	0.62	2.93 ± 3.07
	0.14		1.31		0.03		7.28	
	0.13		2.57		0.04		1.82	
Lung	0.13	0.10 ± 0.04	1.76	1.91 ± 0.49	0.07	0.05 ± 0.01	1.90	1.71 ± 0.12
	0.04		1.39		0.04		1.59	
	0.04		0.38		0.03		0.26	
Muscle	0.02	0.03 ± 0.009	0.28	0.31 ± 0.05	0.02	0.02 ± 0.005	0.32	0.25 ± 0.06
	0.04		0.27		0.02		0.18	
	0.07		3.59		0.04		3.09	
Bone + Marrow	0.05	0.05 ± 0.02	3.50	3.25 ± 0.42	0.01	0.03 ± 0.01	2.55	2.71 ± 0.26
	0.03		2.65		0.03		2.51	

*$MR^{-/-}$ and $MR^{+/+}$ mice received 1 mg/kg P-GUS weekly for 3 wk.

mice. The increased activity with increasing dose likely reflects increased accessibility of MPR in these tissues, because P-GUS initially saturates the MPR in liver and persists much longer in the circulation of $MR^{-/-}$ mice (see Fig. 1 and Table 1). Fig. 5, which is published as supporting information on the PNAS web site, shows histochemical localization of GUS activity in $MR^{+/+}$ and $MR^{-/-}$ mice treated with increasing enzyme doses.

Comparison of Effectiveness of P-GUS in Reducing Lysosomal Storage in $MR^{+/+}$ and $MR^{-/-}$ Mice. $MR^{-/-}$ and $MR^{+/+}$ mice were infused i.v. with 1 mg/kg P-GUS weekly for 3 wk and killed 7 days later for histopathology, histochemistry, and measurement of residual enzyme levels in each organ. We have used this protocol previously to demonstrate differences in effectiveness between P- and NP-GUS and between GUS and GUS-glycosylation-independent lysosomal targeting in $MR^{+/+}$ mice (6, 15). This dose is also comparable to that used in many human ERT trials (2–5).

Untreated $MR^{-/-}$ and $MR^{+/+}$ MPS VII mice were morphologically indistinguishable (Fig. 3) and had lysosomal storage identical to that described in MPS VII/B6 mice (16). In enzyme-treated mice, the liver (Fig. 3), spleen, bone marrow, and renal tubular epithelial cells (not shown) had similar moderate to marked reduction in lysosomal storage in both $MR^{+/+}$ and $MR^{-/-}$ mice. The brain and meninges had no reduction in storage in either group. However, the visceral epithelial cells of the glomeruli, the retinal pigment epithelium, and the osteoblasts lining the rib cortical bone all showed less lysosomal distention in $MR^{-/-}$ than in $MR^{+/+}$ mice (Fig. 3).

Table 4 shows the residual enzyme content in tissues from the above experiment, i.e., 7 days after the third infusion. $MR^{-/-}$ livers showed slightly more enzyme than $MR^{+/+}$ livers, whereas the opposite was true in livers 24 h after infusion where $MR^{-/-}$ mice had ≈83% of the amount present in $MR^{+/+}$ mice (Table 2). These results are not contradictory. The results at 24 h reflect the loss of MR-mediated uptake by Kupffer cells in $MR^{-/-}$ mice, partially compensated by increased MPR-mediated delivery to hepatocytes (6). The 7-day reversal could be explained by the more rapid turnover in Kupffer cells than hepatocytes in $MR^{+/+}$ mice, which leads to a lower total amount of residual enzyme in $MR^{+/+}$ liver at 7 days. The spleen, which normally expresses MR abundantly on macrophages, shows 50% less residual enzyme in $MR^{-/-}$ than in $MR^{+/+}$ mice. On the other hand, in the heart, there is 60% more GUS in $MR^{-/-}$ mice, and in skeletal muscle, there is a smaller increase.

Fig. 4 presents the histochemical staining for GUS 1 wk after the last enzyme infusion. The kidney of $MR^{-/-}$ mice showed a small amount of histochemical staining in the glomeruli, but $MR^{+/+}$ mice showed no staining in kidney. In liver, Kupffer cells still contained more enzyme than hepatocytes in $MR^{+/+}$ mice, whereas $MR^{-/-}$ mice had more diffuse activity, especially in hepatocytes. The spleen in $MR^{+/+}$ mice showed diffuse red pulp GUS activity, whereas staining in $MR^{-/-}$ is limited to red pulp perifollicular cells.

Discussion

MR-null mice have no obvious phenotype other than elevated serum lysosomal enzymes related to slower clearance of serum glycoproteins, including the acid hydrolases (10). When crossed on an MPS VII background, the MR null allele had no additional effect on the phenotype of the MPS VII mouse. The doubly deficient mouse allowed comparison of the MR- and MPR-dependent components of the clearance of infused GUS. At doses of enzyme up to 6.4 mg/kg, the MR clearance system predominated in $MR^{+/+}$ mice. Even at 6.4 mg/kg, the MR-dependent clearance system was barely saturated. The $t_{1/2}$ of

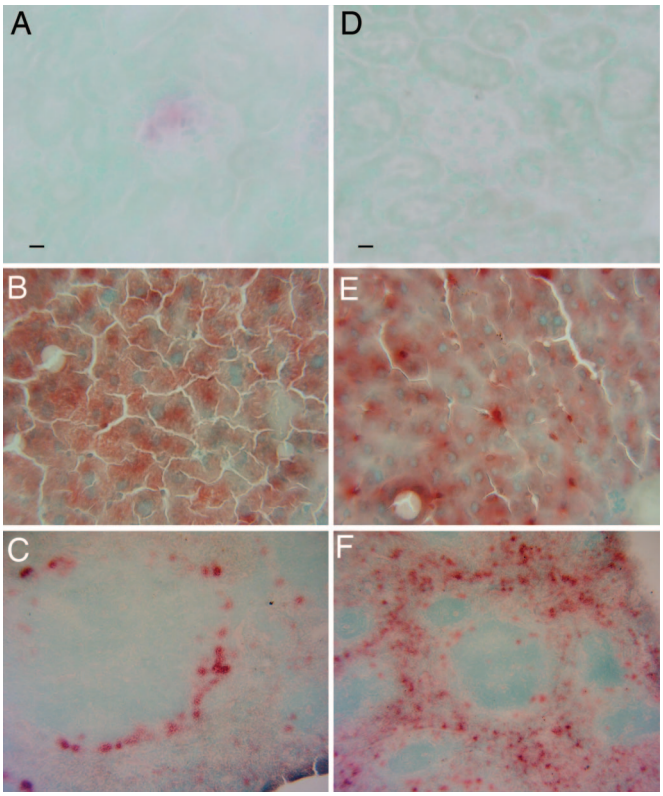

Fig. 4. Histochemical staining for GUS performed 1 wk after the last 1 mg/kg enzyme infusion in $MR^{-/-}$ (*A–C*) and $MR^{+/+}$ (*D–F*) mice. The kidney of the $MR^{-/-}$ mice (*A*) showed a small amount of histochemical staining in the glomeruli, but $MR^{+/+}$ mice (*D*) showed no enzyme activity in kidney. $MR^{-/-}$ mice (*B*) had diffuse enzyme activity in liver, especially in hepatocytes, but $MR^{+/+}$ mice (*E*) contained enzyme in Kupffer cells and hepatocytes. $MR^{-/-}$ mice (*C*) showed reduced enzyme in spleen overall but intense staining in the perifollicular cells, whereas $MR^{+/+}$ mice (*F*) showed more GUS activity diffusely distributed in red pulp (also see spleen data in Table 4). (Scale bar: 6-bromo-2-hydroxy-β-glucuronide, 20 μM.)

clearance of P-GUS was 5 min at 0.2 mg/kg, 7 min at 3.2 mg/kg, and 9 min at 6.4 mg/kg. Eliminating the MR component greatly prolonged clearance of P-GUS and showed that the MPR-mediated clearance system saturated at lower doses ($t_{1/2}$ of 10 min for $MR^{+/+}$ mice and 42 min for $MR^{-/-}$ mice at 6.4 mg/kg).

We had hypothesized that elimination of the MR clearance system would shift a large fraction of enzyme normally targeted to liver to MPR-expressing parenchymal cells in other organs. In fact, ablation of the MR clearance system reduced the amount of enzyme targeted to liver far less than we expected. The fraction of enzyme found in liver 1 h after injection of 1 mg/kg was 38.6% in the $MR^{-/-}$ mouse and 41.8% in the $MR^{+/+}$ mouse. Increasing the enzyme dosage did not alter the relative proportion of enzyme delivered to liver. The ratio of enzyme activity in liver in $MR^{-/-}$ mice was 0.82–0.85 that in $MR^{+/+}$ mice 24 h after infusion of up to 6.4 mg/kg (Table 2). What was altered substantially was the distribution of enzyme in liver, which was shifted predominantly to hepatocytes in $MR^{-/-}$ mice. These experiments indicate that a large fraction of total MPR available to infused P-GUS resides in liver, which gets nearly the same fraction of enzyme even in the absence of the MR. Kupffer cells in $MR^{-/-}$ mice still received some enzyme, because they also express the MPR.

While completely eliminating the MR clearance system (i.e., $MR^{-/-}$ vs. $MR^{+/+}$) reduced uptake by liver by $<18\%$, it still enhanced the effectiveness of P-GUS in clearing storage in kidney, bone, and retina at 1 mg/kg, the dose used in many conventional ERT trials. These observations suggest that one could achieve wider distribution and enhanced clearance of storage by MPR-targeted enzyme if one could block the MR clearance system pharmacologically with an inhibitor. In fact, Ioannou *et al.* (7) reported wider distribution of infused α-galactosidase after preinfusion of yeast mannans, which bind the MR and act as competitive inhibitors (17). Yeast mannans are too toxic and immunogenic for clinical use as inhibitors. However, most recombinant enzymes produced in CHO cells are themselves competitive ligands for the MR, because they contain oligosaccharides with exposed mannose residues as well as phosphorylated oligosaccharides. Using a high enough dose of recombinant enzyme might be a nontoxic way to saturate the MR clearance system and enhance MPR-mediated enzyme delivery. Favorable effects in overcoming the blood–brain barrier to ERT in certain parts of the CNS with high doses of infused GUS may have been partially attributable to saturation of the MR clearance system (18–21).

Another interesting question is the mechanism of eventual clearance of NP-GUS from plasma in the $MR^{-/-}$ mouse. Although the clearance of NP-GUS is greatly slowed ($t_{1/2}$ of 4 h), $>90\%$ of the enzyme is cleared in 24 h (data not shown). Possibly, this very slow clearance is mediated by nonspecific fluid-phase pinocytosis or by adsorptive endocytosis after binding of the enzyme to cell surface proteoglycans, like heparan sulfate. We previously demonstrated that the chimeric enzyme containing the highly basic peptide, TAT, binds cell surface proteoglycans and is taken up by adsorptive endocytosis (22).

Du *et al.* (23) recently reported related studies in which they found that lysosomal acid lipase (LAL) prepared in *Pichia pastoris*, which normally targets the MR in $MR^{+/+}$ mice, is taken up by hepatocytes in the $LAL^{-/-}/MR^{-/-}$ doubly deficient mouse (but not in the $LAL^{-/-}/MR^{+/+}$ mouse) after i.p. injection. These observations led them (23) to propose an uptake mechanism in hepatocytes, independent of the classical MR and MPR, which remains to be identified. This system was observable only if the rapid clearance by the MR was eliminated.

Another striking and unexpected observation was the staining activity in perifollicular cells in the spleens of P-GUS-treated $MR^{-/-}$ mice (Figs. 4 and 5). This staining was even more intense after infusion of NP-GUS (data not shown). The greater intensity in $MR^{-/-}$ mice could be attributable to the much longer exposure to circulating enzyme ($t_{1/2}$ of 4 h). Nonetheless, the preferential localization in these cells indicates a selective uptake system that does not rely on the classical MR or the MPR. The nature of this uptake system remains to be established. These cells could be enriched in cell surface proteoglycans that mediate adsorptive endocytosis of the bound enzyme. Another possible candidate for mediating this uptake would be the recently discovered fourth member of the MR family, Endo180, which is reported to be expressed on fibroblasts, endothelial cells, and macrophages (24).

Materials and Methods

MPS VII/E540A^{Tg} mice are deficient in mouse GUS activity but produce a low level of inactive hGUS protein that confers immunologic tolerance to infused hGUS (9). These mice were bred with an MR-deficient mouse strain (10) to produce the MPS VII/$MR^{-/-}$ mouse that is mouse GUS-deficient, hGUS-tolerant, and MR-deficient. Mice were screened for all three markers (MPS VII, the human GUS E540A transgene, and MR) by PCR primers by using tail DNA to confirm their genotype before use in the experiments described. PCR primers and conditions were as described (9, 10).

Recombinant phosphorylated hGUS (P-GUS) was produced in CHO cells, and enzyme secreted into conditioned medium was collected and purified as described (18). This enzyme contains

the M6P recognition marker and exhibits a K_{uptake} value of 1.5 nM, as measured in human MPS VII fibroblasts. Two nonphosphorylated forms of recombinant hGUS were produced, one (NP-GUS) in a baculovirus/SF 21 insect cell expression system (6) and the second (AP-GUS) by treatment of P-GUS with recombinant human placental AP (12). Both NP- and AP-GUS lack the M6P recognition marker and exhibit essentially no uptake by human fibroblasts. Production and characterization of AP-GUS are described in *Supporting Text*, which is published as supporting information on the PNAS web site.

For plasma clearance experiments, weight-based enzyme doses were determined immediately before each injection. Aliquots of P- or NP-GUS were infused in 125 μl of 10 mM Tris, pH 7.5/150 mM NaCl/1 mM β-glycerophosphate into tail veins of MPS VII/$MR^{+/+}$ or MPS VII/$MR^{-/-}$ mice. Timed 50-μl blood samples obtained by orbital bleed using heparinized hematocrit tubes were centrifuged and plasma assayed for GUS activity on 4-methyl umbelliferyl β-D-glucuronide (25).

Tissue distribution of GUS was determined after enzyme infusion. For tissue distribution at 24 h, mice were infused with 0.4, 1.6, and 6.4 mg/kg GUS in triplicate. Twenty-four hours after infusion, mice were killed and perfused with 25 ml of cold 10 mM Tris, pH 7.2/140 mM NaCl. Tissues were then harvested and frozen in liquid nitrogen. Tissues were thawed and homogenized by Polytron and sonication in 10–30 volumes of cold 10 mM Tris, pH 7.2/140 mM NaCl/1 mM PMSF. Aliquots of total homogenate were assayed for GUS as described above and for protein (26). Tissues were also obtained for histochemical analysis.

To determine the fraction of infused enzyme delivered to liver, $MR^{+/+}$ ($n = 3$) and $MR^{-/-}$ ($n = 2$) mice received 1 mg/kg i.v. P-GUS. Plasma was collected 1 h later, and mice were killed after perfusion, as above. The livers were homogenized, and the fraction of infused GUS in liver was calculated.

To determine tissue GUS levels and the effectiveness of the clearance of MPS storage after multiple infusions, three mice each of both $MR^{+/+}$ and $MR^{-/-}$ strains were infused with 1 mg/kg GUS 1× weekly for 3 wk. Seven days after the last infusion, mice were killed, tissues for GUS assay were frozen in liquid nitrogen, and the samples were processed for histochemical analysis for GUS activity and histological analysis of lysosomal storage (6, 18).

We thank Dr. Michel Nussensweig (The Rockefeller University, New York, NY) for generously providing breeding pairs of $MR^{-/-}$ mice; Colleen Isele and Timothy Becker for excellent technical assistance in management of the mouse colonies and animal husbandry; and Drs. Emil Kakkis, Jung-San Huang, and Mark Sands for helpful critical comments on the manuscript. This work was supported by National Institutes of Health Grant GM34182 (to W.S.S.).

1. Neufeld EF, Muenzer J (2001) in *The Metabolic and Molecular Bases of Inherited Disease*, eds Scriver CR, Beaudet AL, Sly WS, Valle D (McGraw-Hill, New York), pp 3421–3451.
2. Desnick RJ (2004) *J Inherit Metab Dis* 27:385–410.
3. Brady RO, Barton NW (1996) *Lipids* 31 Suppl, S137–S139.
4. Kakkis ED, Muenzer J, Tiller GE, Waber L, Belmont J, Passage M, Izykowski B, Phillips J, Doroshow R, Walot I, *et al.* (2001) *N Engl J Med* 344:182–188.
5. Harmatz P, Giugliani R, Schwartz I, Guffon N, Teles EL, Miranda MC, Wraith JE, Beck M, Arash L, Scarpa M, *et al.* (2006) *J Pediatr* 148:533–539.
6. Sands MS, Vogler CA, Ohlemiller KK, Roberts MS, Grubb JH, Levy B, Sly WS (2001) *J Biol Chem* 276:43160–43165.
7. Ioannou YA, Zeidner KM, Gordon RE, Desnick RJ (2001) *Am J Hum Genet* 68:14–25.
8. Vogler C, Barker J, Sands MS, Levy B, Galvin N, Sly WS (2001) *Pediatr Dev Pathol* 4:421–433.
9. Sly WS, Vogler C, Grubb JH, Zhou M, Jiang J, Zhou XY, Tomatsu S, Bi Y, Snella EM (2001) *Proc Natl Acad Sci USA* 98:2205–2210.
10. Lee SJ, Evers S, Roeder D, Parlow AF, Risteli J, Risteli L, Lee YC, Feizi T, Langen H, Nussenzweig MC (2002) *Science* 295:1898–1901.
11. Kaplan A, Achord DT, Sly WS (1977) *Proc Natl Acad Sci USA* 74:2026–2030.
12. Talkad V, Sly WS (1983) *J Biol Chem* 258:7345–7351.
13. Natowicz MR, Chi MM, Lowry OH, Sly WS (1979) *Proc Natl Acad Sci USA* 76:4322–4326.
14. Natowicz M, Baenziger JU, Sly WS (1982) *J Biol Chem* 257:4412–4420.
15. LeBowitz JH, Grubb JH, Maga JA, Schmiel DH, Vogler C, Sly WS (2004) *Proc Natl Acad Sci USA* 101:3083–3088.
16. Vogler C, Birkenmeier EH, Sly WS, Levy B, Pegors C, Kyle JW, Beamer WG (1990) *Am J Pathol* 136:207–217.
17. Achord DT, Brot FE, Bell CE, Sly WS (1978) *Cell* 15:269–278.
18. Vogler C, Levy B, Grubb JH, Galvin N, Tan Y, Kakkis E, Pavloff N, Sly WS (2005) *Proc Natl Acad Sci USA* 102:14777–14782.
19. Dunder U, Kaartinen V, Valtonen P, Vaananen E, Kosma VM, Heisterkamp N, Groffen J, Mononen I (2000) *FASEB J* 14:361–367.
20. Roces DP, Lullmann-Rauch R, Peng J, Balducci C, Andersson C, Tollersrud O, Fogh J, Orlacchio A, Beccari T, Saftig P, *et al.* (2004) *Hum Mol Genet* 13:1979–1988.
21. Matzner U, Herbst E, Hedayati KK, Lullmann-Rauch R, Wessig C, Schroder S, Eistrup C, Moller C, Fogh J, Gieselmann V (2005) *Hum Mol Genet* 14:1139–1152.
22. Orii KO, Grubb JH, Vogler C, Levy B, Tan Y, Markova K, Davidson BL, Mao Q, Orii T, Kondo N, *et al.* (2005) *Mol Ther* 12:345–352.
23. Du H, Levine M, Ganesa C, Witte DP, Cole ES, Grabowski GA (2005) *Am J Hum Genet* 77:1061–1074.
24. Isacke CM, van der GP, Hunter T, Trowbridge IS (1990) *Mol Cell Biol* 10:2606–2618.
25. Glaser JH, Sly WS (1973) *J Lab Clin Med* 82:969–977.
26. Lowry OH, Rosebrough NJ, Farr AL, Randall RJ (1951) *J Biol Chem* 193:265–275.